# Influence of photoanisotropies on light-controllable structuration of azopolymers surface

*Biagio Audia* [†], *Pasquale Pagliusi* [*,†,§], *Clementina Provenzano*[†], *Alejandro Roche* [‡], *Luis Oriol* [‡] *and Gabriella Cipparrone* [†]

[†] Dipartimento di Fisica, Università della Calabria, Ponte P. Bucci, Cubo 33B, 87036 Rende (CS), Italy

[§] CNR-Nanotec, Ponte P. Bucci 33B, 87036 Rende (CS), Italy

‡ Departamento de Química Orgánica, Instituto de Ciencia de Materiales de Aragón Universidad de Zaragoza-CSICC/Pedro Cerbuna 12, 50009 Zaragoza, Spain

**KEYWORDS**

surface relief gratings, azopolymers, polarization light patterns, photoinduced birefringence, holographic recording, optical gradient force.

**ABSTRACT**

The capability to optically control surface structuration of azopolymer films is an important goal in different research fields, enabling remote activation and tuning of associated processes mediated by the surface. In this work, two amorphous azopolymers, structurally engineered in order to exhibit linear and circular photo-induced optical anisotropies, have been investigated, with the aim to design complex light-reconfigurable topographical structures. Different intensity and polarization patterns were generated by two- or four-beams interferometry and inscribed on the polymer films. Relief depths in the range of hundreds of nanometers have been produced, mediated by the bulk photoinduced anisotropies of the materials. It is shown that, based on the kind of light patterns (intensity and/or polarization), depth and shape of the relief grating can be tuned. Polymers with higher photoinduced birefringences enable to produce deeper reliefs. Bidimensional light polarization patterns generate complex surface structures, even with chiral features, envisaging the possibility to engineer large area opto-controllable surfaces and platforms.

- **INTRODUCTION**

Azopolymers, i.e. responsive polymers able to experience significant structural changes under light irradiation, have been largely investigated in the last twenty years [1-5]. Due to the structural modification occurring under light irradiation, these polymers represent an interesting class of materials which allows remote control of their bulk and surface properties in an easy and flexible way.[6-8] Photoinduced isomerization of the azobenzene units[9] can produce cooperative processes able to induce supramolecular orientation in the materials bulk and even mass transport, thus generating surface modifications.[10-19] These phenomena affect the optical properties,[10,20-24] as well as the topography[25-28] of a polymeric film, enabling to record even more complex light architectures by properly designed writing optical field.[29,30] These photochromic materials are not only sensitive to the intensity of the light, but also to its vectorial nature. Based on this property, complex optical field configurations, with properly designed intensity, phase and polarization, can be exploited for holographic recording,[31] hence providing a new level in the range of light-induced textures in azopolymer film bulk and surface. The reversibility of the photoinduced processes involved in these materials adds another interesting feature: the re-configurability, i.e. the possibility to reinitialize them through thermal or optical treatment. Such feature enables to perform dynamical control of azopolymer based devices.[32] Due to these peculiarities, they were firstly investigated for reconfigurable optical storage and holographic interferometry applications in the optical and optoelectronics research areas.[33-36] Nevertheless, more recently these photoresponsive materials have attracted great attention in the field of surface engineering, as for example, for biomedical applications, ranging from tissue engineering to cell culture investigations.[32, 37-40] Mechanical stimulations are at the basis of several biological mechanisms (growth, migration and invasion, cell differentiation, and tissue-level organization). Cells are mechanically influenced by the substrate both because of its molecular composition and of its

larger scale structure, such as roughness in term of stripes or valleys of different size and shape, or the variation in density and rigidity.[41,42] An extremely powerful technique to exploit mechano-sensing is the engineering of substrate topographies.[43] Therefore, micro and nanofabrication of substrates is an effective tool to explore and control the interface interactions, and has been recently employed in case of cell-substrate biophysical interactions, which allows addressing cell adhesion, migration, proliferation and differentiation.[37,40-42] The most used techniques to fabricate micro and nanometric patterns are micromachining, photo- and soft-lithography. Most of the micro- and nano-structures available presently, exploiting the above cited techniques, suffers on the incapability to be mechanically tuned. In fact, they have fixed topographies that cannot be modified, after manufacturing. Such feature constitutes a limitation in investigating time- or space-varying effects of the substrate on the mediated mechanisms. In this regard, the clear advantage offered by photosensitive materials, like azopolymers, relies on the ability to remotely and dynamically control a wide range of physical and chemical properties of the surfaces in response to light. Then they can be used to perform the optical tuning of the interface and in case of bio-interfaces, for example, enable remote control of the relationship between cells and substrate morphology as well as investigation of dynamical effects. In this regard, light is an ideal triggering tool, as allows a clean, non-damaging and highly localized control. Since the first works in the nineties, optically induced mass transport in azopolymer films has been implemented to generate reconfigurable topographical patterns (surface relief gratings, SRGs), with depth in the nano-/micro-meter range depending on the light configuration (intensity, phase and polarization) and optical geometry of the interfering beams.[10,11,33,34] Bulk modifications are also induced giving additional contributions related to the optical properties of the light structured materials (i.e., linear and/or circular dichroism and birefringence supramolecular chirality). Being polarization sensitive

materials, in fact, light patterns (intensity and polarization) can be recorded as SRGs and/or refractive index modulation enabling a very large variety of structures, with easily controllable length scales. However, the complete understanding of the processes involved in the surface deformation is still an open question, widely discussed by the scientific community.[44-51] Recently, we have reported on a theoretical model based on the optically induced gradient force that includes both the spatial distribution and the anisotropy of the material permittivity occurring during the holographic recording. Experimental results on SRGs recorded by vectorial holography well support theoretical predictions, suggesting that bulk effects, as cooperative photo-orientation and connected photoinduced optical anisotropies, affect the SRG shape and depth[52] when uniform light distribution induces photo-fluidization[13,53] of the material on the whole irradiated area.

Here, we report an investigation of surface patterning of two amorphous poly-methacrylates,[54] induced by the irradiation of polymers films with 1D and 2D polarization and intensity light patterns. Such materials exhibit photoinduced structural and supramolecular modifications, which are strongly correlated to the light polarization, i.e. major axis orientation and elicity, and have demonstrated both linear and circular photoinduced optical anisotropies. Comparative investigation of 1D patterns shows that irradiation with intensity patterns enables to control the depth of the reliefs by controlling the azimuthal angle of the parallel linearly polarized beams with respect to the grating wavevector; while in case of polarization patterns it is possible to affect also the shape and the periodicity. Indeed, the reliefs obtained for the same recording condition exhibit depth values that can be related to the photoinduced optical anisotropies, as predicted by a recently developed theoretical model for SRGs formation.[52] A spatial light modulator (SLM)-assisted holographic technique has been exploited to generate 2D light patterns with pure polarization modulation, to perform complex and single-step structuration of the azopolymers surface. Chiral

traits come out in the surface morphology, where spiral holes and zig-zag shaped relief patterns are induced.

- **EXPERIMENTAL SECTION**

**Materials and Methods** The amorphous azopolymers used for the present investigation are two polymethacrylates synthesized by a modular approach based on the post-polymerization functionalization of a common polymeric skeleton having a degree of polymerization of about 100.[24] The first one is characterized by a dimeric repeating unit based on a 2,2-bis(hydroxymethyl)propionic acid connector containing the 4-cyanoazobenzene and 4-cyanobiphenyl calamitic moieties linked through ester groups (figure 1, P-eCNB/eAZO); in the second polymers, the 4-cyanobiphenyl unit has been replaced by the 4-cyanotolane unit connected by a carbamate linking group instead of the ester one (figure 1, P-cTOL/eAZO). Both polymers have a similar average molar mass as derived from the same parent polymeric skeleton (n approx. 100) and a low dispersity (1.18).[24]

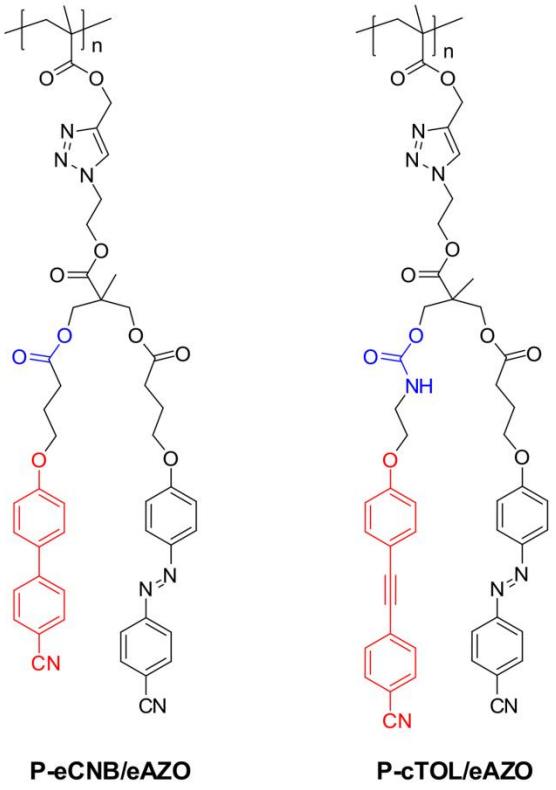


**Figure 1** Chemical structures of the azo-polymers

These polymers have been properly engineered in order to give a high photo-response in term of photo-induced optical anisotropies (linear and circular birefringence) and related opto-mechanical processes inducing surface structuring. [19, 24, 52, 54] The photo-induced birefringences measured by a pump-probe technique and a modelling based on the Stokes–Mueller matrix approach, are reported in the ref. 54. Linear and circular birefringences reach comparable values, which are different for the two polymers: $\Delta n_{lin} = \Delta n_{cir} = (8 \pm 2) * 10^{-3}$ for P-eCNB/eAZO, $\Delta n_{lin} = \Delta n_{cir} = (4 \pm 2) * 10^{-3}$ for P-cTOL/eAZO. The samples are prepared by melting the polymers at 120°C, well above the $T_g$ (54°C and 64°C for P-eCNB/eAZO and P-cTOL/eAZO, respectively), between two glass plates. After cooling them down to room temperature, one of the confining

plates is removed, obtaining μm-thick films (in the range 5-20 μm) with a flat free surface. The polymer films are exposed to 1D intensity or polarization light patterns obtained by the interference of two, equally intense, coherent Gaussian beams ($\lambda_{pump}$ = 457.9nm, $Ar^+$ laser Innova 90C, Coherent Inc.), with parallel linear polarizations (PLPs), i.e. SS, 45° and PP, or orthogonal linear (OL(θ)) and circular (OC) polarizations, according to the geometries in figure 2.[52] Exploiting the Jones-vector formalism, the interference electric field of the PLPs is

$$\vec{E}_{PLP}(\theta) = \vec{E}_r + \vec{E}_s = \begin{bmatrix}\cos\theta \\ \sin\theta\end{bmatrix} e^{i\delta} + \begin{bmatrix}\cos\theta \\ \sin\theta\end{bmatrix} e^{-i\delta} = \begin{bmatrix}\cos\theta \\ \sin\theta\end{bmatrix} 2\cos\delta \qquad 1)$$

with $\theta = 0°, 45°, 90°$ with respect to the incidence plane for the PP, 45° and SS configurations, respectively, while for the OL(θ) and OC polarization patterns are

$$\vec{E}_{OL}(\theta) = \begin{bmatrix}\cos\theta \\ \sin\theta\end{bmatrix} e^{i\delta} + \begin{bmatrix}-\sin\theta \\ \cos\theta\end{bmatrix} e^{-i\delta} = \begin{bmatrix}\cos\delta\,(\cos\theta - \sin\theta) + i\sin\delta\,(\cos\theta + \sin\theta) \\ \cos\delta\,(\cos\theta + \sin\theta) - i\sin\delta\,(\cos\theta - \sin\theta)\end{bmatrix} \qquad 2)$$

and

$$\vec{E}_{OC} = \frac{1}{\sqrt{2}}\begin{bmatrix}1 \\ -i\end{bmatrix} e^{i\delta} + \frac{1}{\sqrt{2}}\begin{bmatrix}1 \\ i\end{bmatrix} e^{-i\delta} = \sqrt{2}\begin{bmatrix}\cos\delta \\ \sin\delta\end{bmatrix} \qquad 3)$$

respectively, where $\delta \equiv \pi x/\Lambda$ is half of the phase difference between the two recording beams.

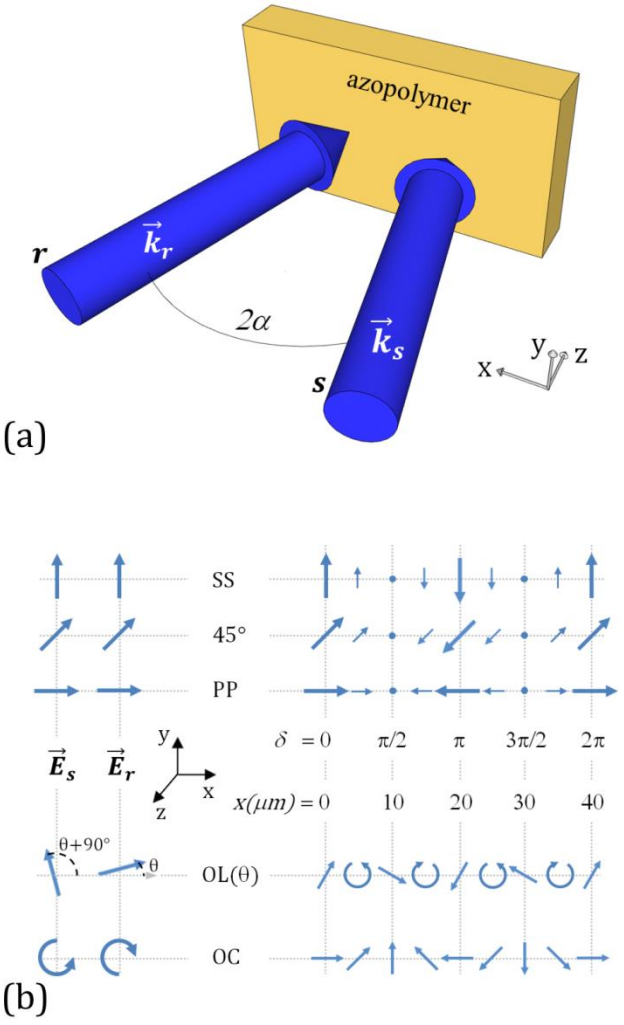


**Figure 2**: (a) Layout of the two-beam holographic recording, in the *xyz* laboratory frame. The wavevectors $\vec{k}_r$ and $\vec{k}_s$ of the interfering beams lie in the *xz* plane and make an angle α with the z axis. The azopolymer film lies in the *xy* plane. (b) Electric field of the intensity and polarization patterns (right side) generated by the interference of PLPs beams (SS, 45° and PP), orthogonal linear (OL(θ)) and circular (OC) polarized beams (left side). The OL(θ) polarization configuration is sketched with the electric field $\vec{E}_r$ ($\vec{E}_s$) oriented at angle θ (θ+90°) with respect to the *xz* plane.

The two beams, having a total intensity of 200mW/cm$^2$, cross at a small angle $2\alpha \cong 1.3°$ yielding an optical periodicity $\Lambda = \lambda_{pump} \,/\, (2\, sin\, \alpha\,) \cong 20\mu m$. The small crossing angle allows for

negligible intensity modulation of the interference optical field obtained by orthogonally polarized beams, while the total field polarization ellipse is approximately confined in the *xy* plane where the grating wavevector lies. In these recording conditions, the SRGs start to develop in few seconds and constantly increase for several minutes. We kept the writing time at 700s. Direct holographic recording of 2D periodic light patterns has been performed by adopting SLM-assisted four beams interferometric geometries. The technique allows to independently set the polarization and the relative phase of the four beams in order to give pure polarization/intensity patterns or mixed ones. Here, we consider the pure polarization patterns produced by the interference of two beam pairs having OC and OL polarization states. In order to avoid intensity modulation, a phase shift of $\pi/2$ is introduced between adjacent beams, as depicted in figures 3b and 3c.[55] The crossing angle of the interfering beams are equal and provide spatial periodicities of the 2D patterns in the range 30-50 μm. The topographies of the polymeric films have been investigated by a profilometer (Veeco Dektak 8) and an atomic force microscope (AFM, Multimode-8 Bruker).

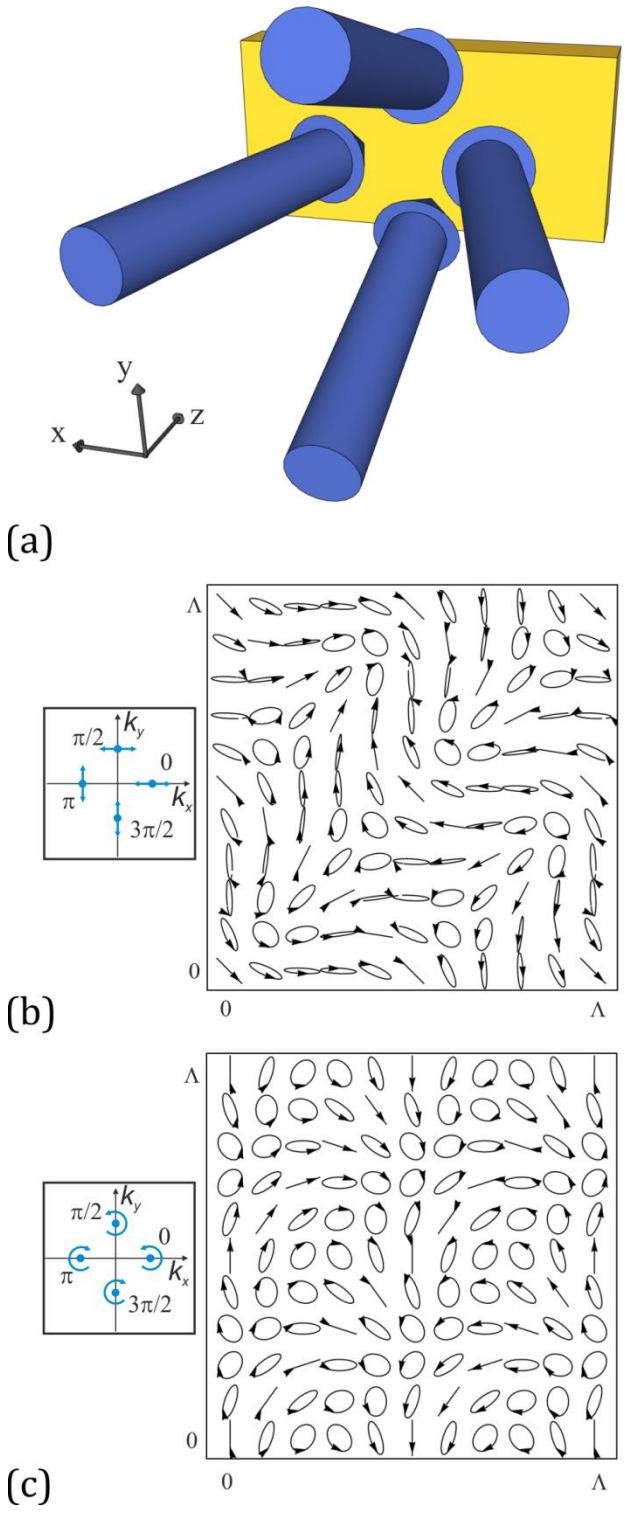


**Figure 3:**(a) Schematization of the four-beam holographic recording, in the *xyz* laboratory frame. Pure 2D polarization patterns are obtained by the interference of four beams with OL (b) and OC

(c) polarization states and a phase difference of π/2 between each consecutive beam. Schemes of the interfering waves in the k-space, showing both polarization and relative phases, are reported beside the polarization interference patterns.

- **RESULTS AND DISCUSSIONS**

In figure 4 are reported the topography profiles of SRGs recorded with intensity patterns obtained by interference of two beams with PLPs, in the PP, 45° and SS configurations (see figure 2).

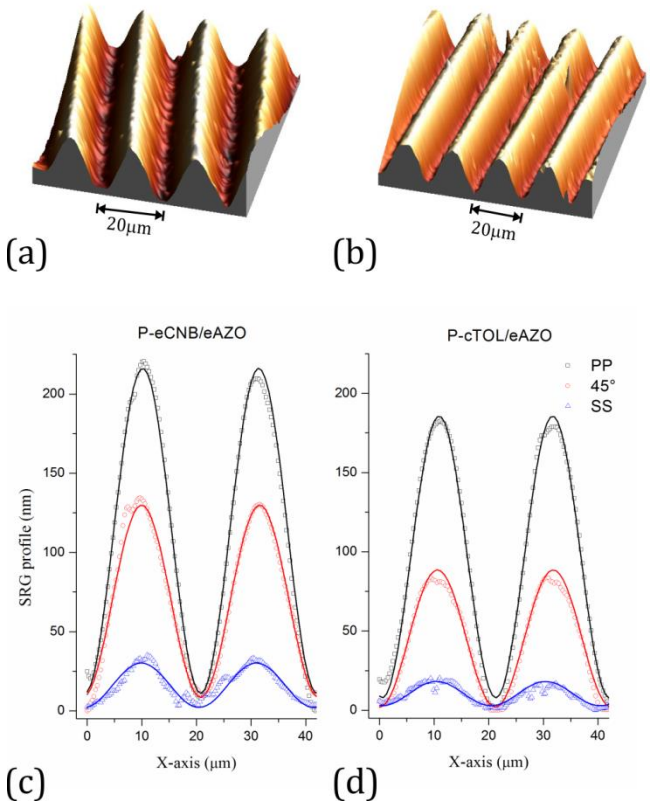


**Figure 4:** AFM surface topographies of the SRGs, generated by the interference of parallel linearly polarized beams at 45°, on (a) P-eCNB/eAZO and (b) P-cTOL/eAZO. Height profiles of the SRGs on (c) P-eCNB/eAZO (16 $\mu m$) and (d) P-cTOL/eAZO (14 $\mu m$) for three different intensity pattern

configurations: PP (black squares), 45° (red circles) and SS (blu triangles). Solid lines represent the sine square fits of the measured profiles.

The measured spatial periodicity of all the SRGs is about 20 μm, equal to the optical periodicity Λ, but the depth of modulation, achieved for the same total intensity (200 mW/cm$^2$) and exposure time (700s), is strongly dependent on the polarization of the light pattern. In particular, the maximum surface modulation depth is measured for the PP configuration: 220 nm for the P-eCNB/eAZO film (16 $\mu m$ thick) and 180 nm for the P-cTOL/eAZO film (14 $\mu m$ thick). It reduces to about half of its maximum value for the 45° PLP (120nm for P-eCNB/eAZO, 90nm for P-cTOL/eAZO) and it becomes much shallower (30nm for P-eCNB/eAZO, 15nm for P-cTOL/eAZO) for the SS configuration. The SRGs are faithfully fitted by a sine square function, according to the intensity profile. In addition, the experimental findings show that the depth of the SRGs can be controlled by tuning the linear polarization of the interference fields, in particular its azimuthal angle with respect to the grating wavevector. According to the expected orientations of the azobenzene unit perpendicular to the light polarization, our results confirm that the photo-driven mass transport responsible of the SRGs formation is more efficient when the chromophores are oriented perpendicular (PP configuration) rather than parallel (SS configuration) to the grating wavevector.[48] Therefore, the main role in SRGs formation is played by orientation phenomena promoted by the chromophores and demonstrate that other diffusive processes connected to the light intensity modulation, as for example the temperature gradient, are less relevant in the process of topographical structuring. In figures 5-7 are reported the analyses of the SRGs recorded by the polarizations patterns sketched in figure 2b, namely OC and OL(θ) configurations for θ=0°, 15°, 30° and 45°. P-eCNB/eAZO films with thicknesses of 6 and 16 $\mu m$ have been used, while for the P-cTOL/eAZO film the thickness is 14 $\mu m$. According to the results and the modelling reported

in the ref.52, the SRGs formation for such kind of pure polarization light patterns can be accounted for via the electromagnetic Lorentz force density, if one includes the photoinduced anisotropies in the electric susceptibility tensor. In particular, the time averaged force density components along the grating wavevector (x component) has been derived for the OC configuration,

$$\langle f_x \rangle_{t,OC} = \left\{ Re\left[\hat{\chi}_0 + 2\hat{k}_{\parallel}\right] 2 \sin 2\delta \right\} \varepsilon_0 \pi / \Lambda \qquad 4)$$

and the OL(θ) configuration,

$$\langle f_x \rangle_{t,OL} = \left\{ -Re\left[\hat{\chi}_0 + 2\hat{k}_{\parallel}\right] 2 \sin 2\delta \sin 2\theta + Re\left[\hat{k}_{\parallel} - \hat{k}_{\perp} - 2\hat{k}_c\right] \sin 4\delta - Im\left[\hat{k}_{\parallel} - \hat{k}_{\perp} - 2\hat{k}_c\right] 2 \cos 4\delta \cos 2\theta \right\} \varepsilon_0 \pi / \Lambda \qquad 5)$$

where $\hat{\chi}_0$ is the intrinsic isotropic and homogeneous complex susceptibility of the material, $\hat{k}_{\parallel}$, $\hat{k}_{\perp}$ and $\hat{k}_c$ are the contributions to the susceptibility due to the nonlinear response to parallel, perpendicular linear polarizations and circular polarization, respectively.[52] In figure 5, the topographic profiles of the SRGs recorded with the OC pattern (figure 2b) are reported for the 16 $\mu m$ thick P-eCNB/eAZO and the 14 $\mu m$ thick P-cTOL/eAZO films. This configuration is the most efficient in terms of surface structuring, and a depth of 400nm for both polymers has been measured. The topography is characterized by a sinusoidal profile with the same spatial periodicity Λ=20 μm of the polarization pattern. According to the driving force density component in eq.4, the SRG formation is mainly affected by the intrinsic susceptibility $\hat{\chi}_0 \gg \hat{k}_{\parallel}$ of the material, which is expected to be similar for the two polymers.

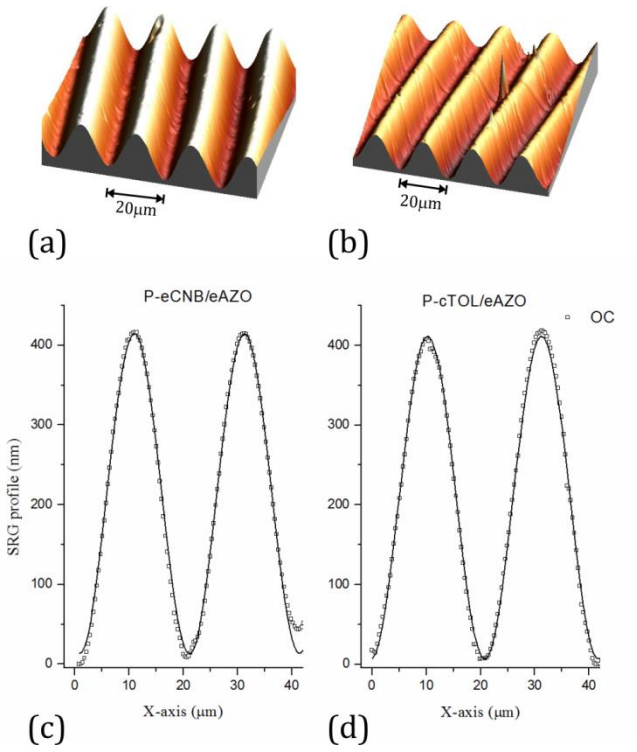


**Figure 5:** AFM surface topographies and height profiles of the SRGs, generated by the interference of OC polarized beams, on (a, c) P-eCNB/eAZO (16 $\mu m$) and (b, d) P-cTOL/eAZO (14 $\mu m$). Solid lines represent the sinusoidal fits of the measured profiles.

In figure 6 we compare the topographic profiles on the 6 $\mu m$ thick P-eCNB/eAZO and 14 $\mu m$ thick P-cTOL/eAZO films, after irradiation with the OL(θ) patterns at different θ values. At θ=0°, which corresponds to the standard SP configuration, a sinusoidal profile occurs with the expected periodicity Λ/2, [48, 49, 52] and a depth of about 100nm for both polymers.

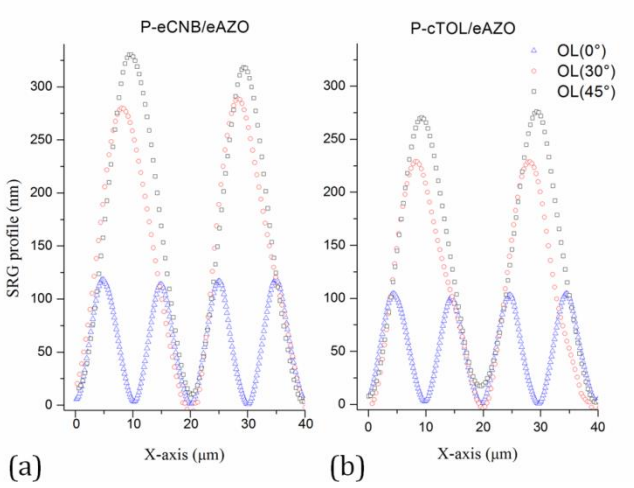


**Figure 6:** Height profiles of the SRGs on (a) P-eCNB/eAZO ($6\mu m$) and (b) P-cTOL/eAZO (14 $\mu m$) recorded by the 1D OL(θ) polarization patterns at different angle θ: 0° (blue triangles), 30° (red circles) and 45° (black squares).

The rotation of the linear polarizations of the interfering beams by θ =15° breaks the symmetry, therefore consecutive peaks of the former profile are enhanced and suppressed, and the SRG spatial periodicity switches from Λ/2 to Λ (figure 7). The depth of the reliefs progressively increases by further increasing θ, and reaches its maximum value for θ=45° for both samples (figure 6), while the relief profile acquires a sinusoidal shape again. It should be noted that in the OL(θ) configuration at different θ values the depth of the SRGs on the 6 $\mu m$ P-eCNB/eAZO film is always higher than the ones on the 14 $\mu m$ P-cTOL/eAZO film. In figure 7 the surface profiles obtained for the OL(θ) configuration at θ =15° are compared for both azopolymers at different thicknesses: 6 $\mu m$ and 16 $\mu m$ P-eCNB/eAZO films (fig.7c), 14 $\mu m$ P-cTOL/eAZO film (fig.7d).

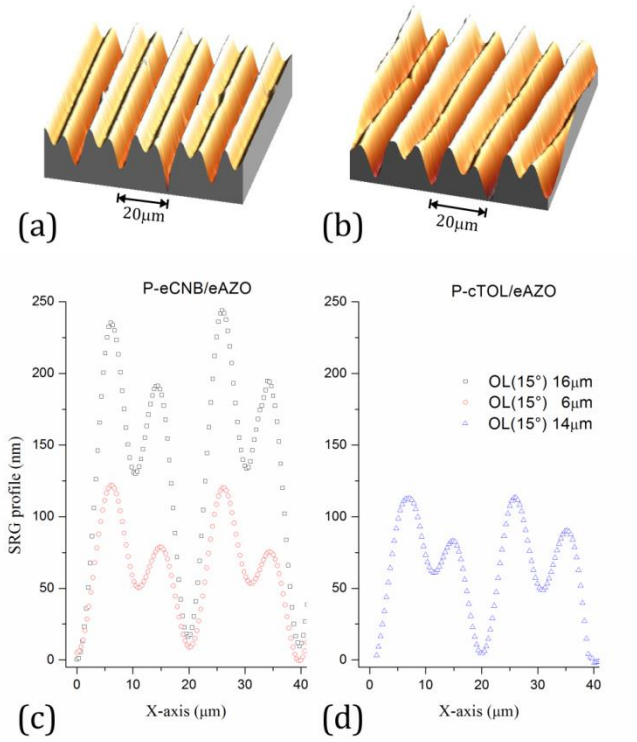


**Figure 7**: AFM surface topographies and height profiles of the SRGs at different film thickness, generated by the interference of OL(θ) polarized beams at θ=15°, on (a, c) P-eCNB/AZO and (b, d) P-cTOL/AZO. P-eCNB/eAZO: 16 $\mu m$ (black squares) and 6 $\mu m$ (red circles); P-cTOL/eAZO : 14 $\mu m$ (blue triangles)

The reliefs' depth appears to be a growing function of the film thickness, increasing from 120 nm to 220 nm for the P-eCNB/eAZO films (fig. 7c). On the other hand, for comparable film thickness, it is smaller on the P-cTOL/eAZO film (110nm, fig.7d) than on the P-eCNB/eAZO (220nm, black squares in fig.7c), proving that the latter is more efficient in term of SRGs formation. This evidence supports the involvement of the photoanisotropic response of the material in the electromagnetic force density. Indeed, for θ=15°, the effective contribution of the photoresponse $\hat{k}_{\parallel} - \hat{k}_{\perp} - 2\hat{k}_{c}$, involving both linear and circular photoinduced anisotropies, is relevant in eq.5, and an

independent experiment has shown that the linear and circular birefringences for the P-eCNB/eAZO are twice the P-cTOL/eAZO ones.[54]

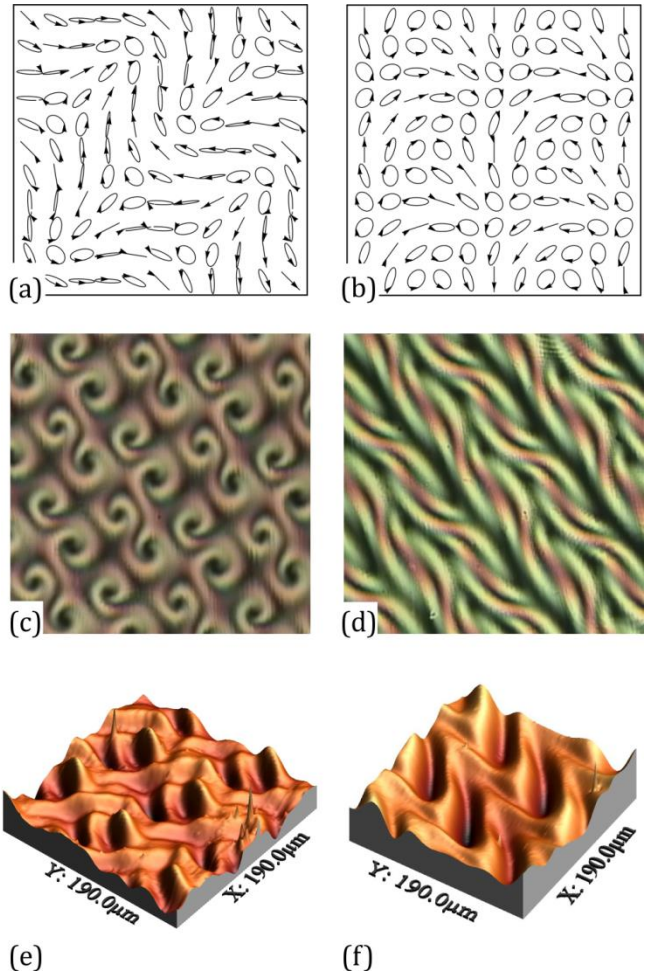


**Figure 8:** Polarizing microscope images between crossed polarizers (c) and (d), and AFM surface topographies (e) and (f) after holographic recording with the 2D polarization patterns (a) and (b) respectively on the P-eCNB/eAZO ($6\mu m$).

The polymer films have been also used to investigate topographical shaping induced by irradiation with the 2D polarization patterns reported in figure 8a and 8b. Both patterns display bidimensional configurations of the optical field where elicity and azimuthal angle spatially varies in the range [1,-1] and [0°,180°], respectively. The π/2 phase shift between each consecutive beam (figure 3)

ensures the absence of intensity modulation in the interference field, then uniform material photo-fluidization occurs under illumination. The optical microscope images between crossed polarizers (fig. 8c and 8d) and the surface topographies (fig. 8e and 8f) of the P-eCNB/eAZO film with thickness 6 $\mu m$ are reported for both OL and OC configurations. Similar results have been obtained for the other polymer samples. The four-beams OL configuration reveals the establishment of a patterned spiral-like supramolecular arrangement with alternating opposite chirality, as revealed by the photoinduced birefringence in the bulk (fig. 8c). Furthermore, it results in a complex surface topography, where spiral holes alternate to twisted zig-zag reliefs (fig. 8e). On the other hand, the OC configuration displays a ribbon like spatial pattern in the material birefringence (fig. 8d), which corresponds to zig-zag surface reliefs (fig. 8f).

- **CONCLUSIONS**

In conclusion, we have investigated the surface structuring of two amorphous azopolymers structurally engineered in order to exhibit high optical anisotropies, both linear and circular. The photoinduced surface structuration observed on both the azopolymers films follows the optical field distribution of the light pattern, in both amplitude and polarization. Holographic recording based on 1D intensity modulation patterns in the PLPs configurations allows to control the depth of the reliefs by selecting the polarization direction of the light pattern. Pure 1D polarization holographic patterns allow for shape, periodicity and depth control of the SRGs, according to the theoretical model based on the Lorentz force related to the photoinduced anisotropies in the material bulk. OL(θ) configurations are particularly suitable to prove the influence of photoanisotropies in the force density. Indeed, for comparable film thickness, deeper surface reliefs are obtained on polymer exhibiting larger values of the photoinduced linear and circular birefringences. SLM assisted-holographic recording has been employed to demonstrate that more

complex surface textures can be obtained exploiting the capability to suitably design the illuminating light pattern. In this respect, topographic textures of zig-zag shaped reliefs and spiral holes patterns have been created by irradiating the azopolymer film with properly designed 2D pure polarization patterns. The reported results suggest strategies in the design of photo-responsive materials and light patterns, addressed to develop opto-controllable interface able to broaden the range of applications in the fields of surface engineering for biology and photonics.

## AUTHOR INFORMATION


**Corresponding author**

* Email: pasquale.pagliusi@fis.unical.it (Pasquale Pagliusi)

**ORCID**

Pasquale Pagliusi: 0000-0001-8077-816X

Gabriella Cipparrone: 0000-0003-4880-1942

Luis Oriol: 0000-0002-0922-5615


**Notes**

The authors declare no competing financial interest.

## ACKNOWLEDGMENT


Biagio Audia acknowledges POR Calabria FSE/FESR 2014-2020 for financial support.


## REFERENCES

(1) Li, Q. *Intelligent Stimuli-Responsive Materials: From Well-Defined Nanostructures to Applications*. John Wiley & Sons, Hoboken, NJ, **2013**

(2) Aguilar, M. R.; San Román, J. *Smart Polymers and their Applications*. Woodhead Publishing, **2014**

(3) Wei, M.; Gao, Y.; Li, X.; Serpe, M. J. Stimuli-responsive polymers and their applications, *Polym. Chem.* **2017**, 8, 127 - 143

(4) Zhang, Z. *Switchable and Responsive Surfaces and Materials for Biomedical Applications*. Elsevier, **2015**

(5) Stumpe, J.; Kulikovska, O.; Goldenberg, L. M.; Zakrevskyy, Y. *Smart Light-Responsive Materials*. Ed. Y. Zhao and T. Ikeda, John Wiley & Sons Ltd., Hoboken, NJ, USA, **2009**

(6) Vapaavuori, J.; Bazuin, C. G.; Priimagi, A. Supramolecular design principles for efficient photoresponsive polymer–azobenzene complexes. *J. Mater. Chem. C* **2018**, 6, 2168-2188

(7) Oscurato, S.L.; Salvatore, M.; Maddalena, P.; Ambrosio, A. From nanoscopic to macroscopic photo-driven motion in azobenzene-containing materials. *Nanophotonics* **2018**, 7, 1387-1422

(8) Kim, K.; Park, H.; Park, K.J.; Park, S.H.; Kim, H.H.; Lee, S. Light-Directed Soft Mass Migration for Micro/Nanophotonics. *Advanced Optical Materials* **2019**, 1900074

(9) Weigert, F. Photodichroismus und Photoanisotropie I., *Zeitschrift für Physikalische Chemie* **1929** ,3, 377-388

(10) Nikolova, L.; Todorov, T.; Ivanov, M.; Andruzzi, F.; Hvilsted, S.; Ramanujam, P. S. Photoinduced circular anisotropy in side-chain azobenzene polyesters. *Optical Materials* **1997**, 8, 255-258

(11) Viswanathan, N. K.; Balasubramanian, S.; Li, L.; Tripathy, S. K.; J. Kumar. A detailed investigation of the polarization-dependent surface-relief-grating formation process on azo polymer films. *Japanese journal of applied physics* **1999**, 38, 5928

(12) Natansohn, A.; Rochon, P. Photoinduced motions in azo-containing polymers. *Chemical reviews* **2002**, 102, 4139-4176

(13) Yang, K.; Yang, S.; Kumar, J., Formation mechanism of surface relief structures on amorphous azopolymer films. *Physical Review B* **2006**, *73*, 165204.

(14) Shibaev, V.; Bobrovsky, A.; Boiko, N. Photoactive liquid crystalline polymer systems with light-controllable structure and optical properties. *Progress in Polymer Science* **2003**, 28, 729-836

(15) Tejedor, R. M.; Millaruelo, M.; Oriol, L.; Serrano, J. L.; Alcalá, R.; Rodríguez, F. J.; Villacampa, B. Photoinduced supramolecular chirality in side-chain liquid crystalline azopolymers. *Journal of Materials Chemistry* **2006**, 16, 1674-1680

(16) Zhao, Y.; He, J. Azobenzene-containing block copolymers: the interplay of light and morphology enables new functions. *Soft Matter* **2009**, 5, 2686-2693

(17) Hendrikx, M.; Schenning, A.; Debije, M.; Broer, D. Light-triggered formation of surface topographies in azo polymers. *Crystals* **2017**, 7, 231

(18) Karageorgiev, P.; Neher, D.; Schulz, B.; Stiller, B.; Pietsch, U.; Giersig, M.; Brehmer, L. From anisotropic photo-fluidity towards nanomanipulation in the optical near-field. *Nature materials* **2005**, 4, 699

(19) Provenzano, C.; Pagliusi, P.; Cipparrone, G.; Royes, J.; Piñol, M.; Oriol, L. Polarization holograms in a bifunctional amorphous polymer exhibiting equal values of photoinduced linear and circular birefringences. *The Journal of Physical Chemistry B* **2014**, 118, 11849-11854

(20) Sobolewska, A.; Miniewicz, A. On the inscription of period and half-period surface relief gratings in azobenzene-functionalized polymers. *The Journal of Physical Chemistry B* **2008**, 112, 4526-4535

(21) Nikolova, L.; Todorov, T.; Ivanov, M.; Andruzzi, F.; Hvilsted, S.; Ramanujam, P. S. Polarization holographic gratings in side-chain azobenzene polyesters with linear and circular photoanisotropy. *Applied optics* **1996**, 35, 3835-3840, and references therein.

(22) Pagès, S.; Lagugné-Labarthet, F.; Buffeteau, T.; Sourisseau, C. Photoinduced linear and/or circular birefringences from light propagation through amorphous or smectic azopolymer films. *Applied Physics B* **2002**, 75, 541-548

(23) Cipparrone, G.; Pagliusi, P.; Provenzano, C.; Shibaev, V. P. Polarization holographic recording in amorphous polymer with photoinduced linear and circular birefringence. *The Journal of Physical Chemistry B* **2010**, 114, 8900-8904

(24) Royes, J.; Provenzano, C.; Pagliusi, P.; Tejedor, R. M.; Piñol, M.; Oriol, L. A bifunctional amorphous polymer exhibiting equal linear and circular photoinduced birefringences. *Macromolecular rapid communications* **2014**, 35, 1890-1895

(25) Kopyshev, A.; Galvin, C. J.; Patil, R. R.; Genzer, J.; Lomadze, N.; Feldmann, D.; Zakrevski, J.; Santer, S. Light-Induced Reversible Change of Roughness and Thickness of Photosensitive Polymer Brushes. *ACS applied materials & interfaces* **2016**, 8, 19175-19184

(26) Jiang, X. L.; Li, L.; Kumar, J.; Kim, D. Y; Tripathy, S. K. Unusual polarization dependent optical erasure of surface relief gratings on azobenzene polymer films. *Applied Physics Letters* **1998**, 72, 2502-2504

(27) Vapaavuori, J.; Ras, R. H. A.; Kaivola, M.; Bazuin, C. G.; Priimagi, A. From partial to complete optical erasure of azobenzene–polymer gratings: effect of molecular weight. *Journal of Materials Chemistry C* **2015**, 3, 11011-11016

(28) Veer, P. U.; Pietsch, U.; Saphiannikova, M. Time and temperature dependence of surface relief grating formation in polymers containing azobenzene groups with different dipole moment. *Journal of Applied Physics* **2009**, 106, 014909

(29) Ruiz, U.; Pagliusi, P.; Provenzano, C.; Cipparrone, G. Highly efficient generation of vector beams through polarization holograms. *Applied Physics Letters* **2013**, 102, 161104

(30) Hahn, C.; Choi, Y.; Yoon, J. W.; Song, S.H.; Berini, P. Observation of exceptional points in reconfigurable non-Hermitian vector-field holographic lattices. *Nature communications*, **2016**, 7, 12201

(31) Nikolova, L.; Ramanujam, P. S. *Polarization holography*. Cambridge University Press, **2009**, and reference therein.

(32) Chang, V.Y.; Fedele, C.; Priimagi, A.; Shishido, A.; Barrett, C.J. Photoreversible Soft Azo Dye Materials: Toward Optical Control of Bio-Interfaces. *Advanced Optical Materials* **2019**, 7, 1900091.

(33) Brown, D.; Natansohn, A.; Rochon, P. Azo polymers for reversible optical storage Orientation and dipolar interactions of azobenzene side groups in copolymers and blends containing methyl methacrylate structural units. *Macromolecules* **1995**, 28, 6116-6123

(34) Rasmussen, P. H.; P. Ramanujam, S.; Hvilsted, S.; Berg, R. H. A remarkably efficient azobenzene peptide for holographic information storage. *Journal of the American Chemical Society* **1999**, 121, 4738-4743

(35) Shishido, A. Rewritable holograms based on azobenzene-containing liquid-crystalline polymers. *Polymer journal* **2010**, 42, 525

(36) Yager, K.G.; Barrett, C.J. *Smart Light-Responsive Materials*. Chapter17, RSC Publishing: Cambridge, UK, **2008**

(37) Rocha, L.; Paius, C.M.; Luca-Raicu, A.; Resmerita, E.; Rusu, A.; Maleavin, I.A.; Hamel, M.; Branza-Nichit, N.; Hurduc, N. Azobenzene based polymers as photoactive supports and micellar structures for applications in biology. *Journal of Photochemistry and Photobiology A: Chemistry* **2014**, 291, 16-25

(38) Rosales, A. M.; Mabry, K. M.; Nehls, E. M.; Anseth, K.S. Photoresponsive elastic properties of azobenzene-containing poly (ethylene-glycol)-based hydrogels. *Biomacromolecules* **2015,** 16, 798-806

(39) Ruskowitz, E. R.; DeForest, C.A. Photoresponsive biomaterials for targeted drug delivery and 4D cell culture. *Nature Reviews Materials* **2018**, 3, 17087

(40) Fedele, C.; Netti, P. A.; Cavalli, S. Azobenzene-based polymers: emerging applications as cell culture platforms. *Biomaterials science* **2018**, 6, 990-995

(41) Kim, D.H.; Provenzano, P.; Smith, C. L.; Levchenko, A. Matrix nanotopography as a regulator of cell function. *The Journal of cell biology* **2012**, 197, 351-360

(42) Nguyen, A. T.; Sathe, S.R.; Yim, E.K. From nano to micro: topographical scale and its impact on cell adhesion, morphology and contact guidance. *Journal of Physics: Condensed Matter* **2016**, 28, 183001

(43) Mirkin, C.A.; Rogers, J. A. Emerging methods for micro-and nanofabrication. *Materials Research Society Bulletin* **2001**, 26, 506-509

(44) Saphiannikova, M.; oshchevikov, W. T; Ilnytskyi, J. Photoinduced deformations in azobenzene polymer films. *Nonlinear Opt and Quantum Opt* **2010**, 41, 27-57.

(45) Juan, M. L.; Plain, J.; Bachelot, R.; Royer, P.; Gray, S. K.; Wiederrecht, G. P. Multiscale model for photoinduced molecular motion in azo polymers. *ACS nano* **2009**, 3, 1573-1579.

(46) Lefin, C. F. P.; Nunzi, J.-M. Anisotropy of the photo-induced translation diffusion of azobenzene dyes in polymer matrices. *Pure and Applied Optics: Journal of the European Optical Society Part A* **1998**, 7, 71

(47) Ciobotarescu, S.; Hurduc, N.; Teboul, V. How does the motion of the surrounding molecules depend on the shape of a folding molecular motor? *Physical Chemistry Chemical Physics* **2016**, 18, 14654-14661

(48) Yadavalli, N. S.; Santer, S. In-situ atomic force microscopy study of the mechanism of surface relief grating formation in photosensitive polymer films. *Journal of Applied Physics* **2013**, 113, 224304

(49) Sobolewska, A.; Miniewicz, A. On the inscription of period and half-period surface relief gratings in azobenzene-functionalized polymers. *The Journal of Physical Chemistry B* **2008**, 112. 4526-4535

(50) Ambrosio, A.; Marrucci, L.; Borbone, F.; Roviello, A.; Maddalena, P. Light-induced spiral mass transport in azo-polymer films under vortex-beam illumination. *Nature communications* **2012**, 3, 989

(51) Fabbri, F.; Lassailly, Y.; Monaco, S.; Lahlil, K.; Boilot, J. P.; Peretti, J. Kinetics of photoinduced matter transport driven by intensity and polarization in thin films containing azobenzene. *Physical Review B* **2012**, 86, 115440

(52) Pagliusi, P.; Audia, B.; Provenzano, C.; Pinol, M.; Oriol, L.; Cipparrone, G. Tunable surface patterning of azopolymer by vectorial holography: the role of photoanisotropies in the driving force. *ACS applied materials & interfaces* **2019**,11, 34471-34477

(53) Saphiannikova, M.; Toshchevikov, V. Optical deformations of azobenzene polymers: Orientation approach vs. photofluidization concept. *Journal of the Society for Information Display* **2015**, 23, 146-153

(54) Roche, A.; García-Juan, H.; Royes, J.; Oriol, L.; Piñol, M; Audia, B.; Pagliusi, P.; Provenzano, C.; Cipparrone, G. Tuning the Thermal Properties of Azopolymers Synthesized by Post-Functionalization of Poly (propargyl Methacrylate) with Azobenzene Azides: Influence on the Generation of Linear and Circular Birefringences. *Macromolecular Chemistry and Physics* **2018**, 219, 1800318.

(55) Ruiz, U.; Pagliusi, P.; Provenzano, C.; Shibaev, V. P.; Cipparrone G. Smart Materials: Supramolecular Chiral Structures: Smart Polymer Organization Guided by 2D Polarization Light Patterns. *Advanced Functional Materials* **2012**, 22, 2882-2882

For tables of contents use only